Dispersion Characteristics for Wide Slotlines on Low-Permittivity Substrates

R. JANASWAMY AND D. H. SCHAUBERT, SENIOR MEMBER, IEEE

Abstract — **This paper provides additional dispersion data on slotlines not available in the literature to date. In particular, data are presented on wide slots etched on an electrically thin substrate of low-dielectric constant. The range of parameters covered in this paper are $0.006 \leq d/\lambda_0 \leq 0.06$, $0.005 \leq W/\lambda_0 \leq 2.0$, and $\epsilon_r = 2.22, 3.0, 3.8, 9.8$. The problem is formulated using the spectral-domain technique, and the spectral Galerkin's method is employed to compute the slot wavelength. Numerical results are compared to the experimental data over 2–6 GHz for slotlines on a 1.57-mm substrate ($\epsilon_r = 2.55$). Agreement to within 2.0 percent is obtained.**

I. Introduction

Dispersion characteristics of a slotline shown in Fig. 1 have been thoroughly investigated by a number of authors in the past [1]–[6]. Cohn [1] made some elegant approximations essentially valid for narrow slots on high-permittivity substrates, and solved the problem using the transverse resonance technique. Mariani *et al.* [2] presented extensive curves for slot wavelength λ' and characteristic impedance based on the above method. Garg and Gupta [5] obtained closed-form expressions for slot wavelengths and characteristic impedance by curve fitting these numerical data. Itoh and Mittra [3] highlighted a new technique called the spectral-domain technique to solve for the propagation constant of the slotline in a more rigorous manner. Knorr and Kuchler [4] extended the method to solve for the characteristic impedance as well. J. B. Davies and D. Mirshekar-Syahkal [6] applied the spectral-domain technique to a shielded multilayered structure. In all these works, the range of various parameters was restricted to $9.7 \leq \epsilon_r \leq 20.0$, $0.02 \leq W/d \leq 2.0$, and $0.01 \leq (d/\lambda_0) \leq (d/\lambda_0)_{TE_1}$, where $(d/\lambda_0)_{TE_1}$ is equal to the cutoff for the first TE surface wave on a grounded slab. Though this range is quite adequate for a slotline used as a transmission line and for many circuit applications, there is an increasing interest [7]–[9] to modify the slotline for antenna applications, where the above constraints breakdown. In [7], for instance, the slot is flared linearly to a width W of the order of a wavelength and the substrate is thin ($d/\lambda_0 \simeq 0.008$) with $\epsilon_r = 3.0$. It is, therefore, desirable to know the propagation constant of wide slots on these low-ϵ_r substrates.

In this paper, theoretical and experimental data are presented for the slot wavelength λ' for wide slots on low-ϵ_r substrates. The problem is first formulated using the spectral-domain immitance approach suggested by Itoh [10], and expressions are obtained for the two-dimensional dyadic admittance Green's function, which relates the electric surface currents and slot electric field in the plane of the slot. The unknown transverse and longitudinal slot fields are expanded in a set of basis functions, and Galerkin's method [3] together with Parseval's theorem are invoked to result finally in a set of homogeneous equations for the unknown coefficients used in the expansion. The elements of the matrix operating on these coefficients are all functions of the propagation constant k_z along the slotline. The dispersion relation is obtained by solving for values of k_z that render the determinant of the matrix to zero. Finally, comparison is made between the computed and experimentally determined slot wavelength λ'.

Manuscript received December 3, 1984; revised March 18, 1985. This work was supported in part by NASA Langley Research Center under Grant NAG-1-279.

The authors are with the Department of Electrical and Computer Engineering, University of Massachusetts, Amherst, MA 01003.

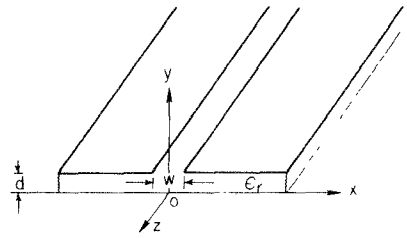

Fig 1. Geometry of slotline.

II. Formulation of the Problem

The method suggested in [10] as applied to the slotline leads to

$$\begin{bmatrix} \tilde{Y}_{xx} & \tilde{Y}_{xz} \\ \tilde{Y}_{zx} & \tilde{Y}_{zz} \end{bmatrix} \begin{bmatrix} \tilde{E}_x(\alpha) \\ \tilde{E}_z(\alpha) \end{bmatrix} = \begin{bmatrix} \tilde{J}_x(\alpha) \\ \tilde{J}_z(\alpha) \end{bmatrix} \tag{1}$$

where $\tilde{E}_x$ and $\tilde{E}_z$ are, respectively, the transverse and longitudinal fields in the slot region, and $\tilde{J}_x$ and $\tilde{J}_z$ are electric surface currents on the metalization. A tilde denotes quantities Fourier transformed with respect to x, and α is the transformed variable. $\tilde{Y}_{xx}$, $\tilde{Y}_{xz}$, $\tilde{Y}_{zx}$, and $\tilde{Y}_{zz}$ are elements of the two-dimensional admittance Green's function given by

$$\tilde{Y}_{xx} = \frac{1}{j\omega\mu_0\gamma_1 T^e T^m} \cdot \begin{bmatrix} [(T^e-1)(\gamma_1+T^m)(2k_z^2-k_0^2(\epsilon_r+1))+(k_z^2-k_0^2) \\ \cdot\{2\epsilon_r\gamma_1-k_0^2 dX_0(\epsilon_r-1)\}-\gamma_1(X_0\alpha k_0 d)^2\epsilon_r(\epsilon_r-1)] \end{bmatrix} \tag{2a}$$

$$\tilde{Y}_{xz} = \tilde{Y}_{zx} = \frac{\alpha k_z}{j\omega\mu_0\gamma_1 T^e T^m} \cdot \begin{bmatrix} 2\epsilon_r\gamma_1 + X_0 d\{2(\epsilon_r+1)\gamma_1^2 - k_0^2(\epsilon_r-1)\} \\ +\gamma_1(X_0 d)^2\{2\gamma_2^2+\epsilon_r(\epsilon_r-1)k_0^2\} \end{bmatrix} \tag{2b}$$

$$\tilde{Y}_{zz} = \frac{1}{j\omega\mu_0\gamma_1 T^e T^m} \cdot \begin{bmatrix} (T^e-1)(\gamma_1+T^m)(2\alpha^2-k_0^2(\epsilon_r+1))+(\alpha^2-k_0^2) \\ \cdot\{2\epsilon_r\gamma_1-k_0^2 X_0 d(\epsilon_r-1)\}-\gamma_1(X_0 dk_z k_0)^2\epsilon_r(\epsilon_r-1) \end{bmatrix} \tag{2c}$$

where $k_0 = \omega\sqrt{\mu_0\epsilon_0}$ is the free-space wavenumber, γ_1, γ_2 are the transverse propagation constants in medium 1 (air) and 2 (dielectric slab), respectively, and where

$$\alpha^2 + k_z^2 = \gamma_1^2 + k_0^2 = \gamma_2^2 + \epsilon_r k_0^2$$

$$X_0 = \tanh(\gamma_2 d)/(\gamma_2 d)$$

$$T^e = 1 + \frac{\gamma_1}{\gamma_2}\tanh(\gamma_2 d)$$

$$T^m = \epsilon_r\gamma_1 + \gamma_2\tanh(\gamma_2 d).$$

The zeros of T^e and T^m give the location in the α plane of the surface waves on a grounded dielectric slab.

E_x and E_z over the slot region are approximated by expanding in a finite set of basis functions.

$$E_x = \sum_1^{M_x} a_n e_n^x \qquad E_z = \sum_1^{M_z} b_n e_n^z.$$

0018-9480/85/0800-0723$01.00 ©1985 IEEE

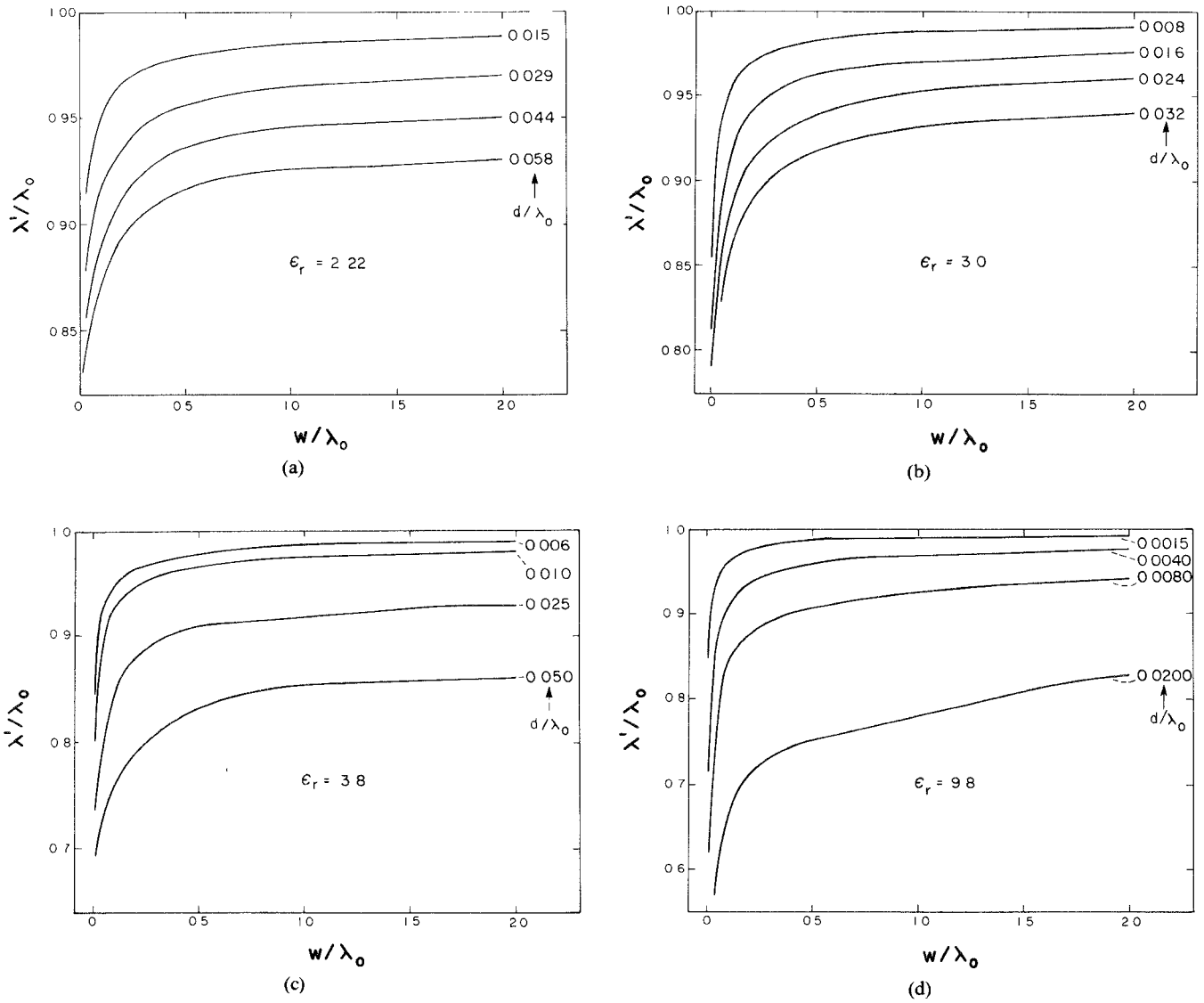

Fig. 2. Normalized slot wavelength. (a) $\epsilon_r = 2.22$. (b) $\epsilon_r = 3.0$. (c) $\epsilon_r = 3.8$. (d) $\epsilon_r = 9.8$.

Employing Galerkin's method in the spectral domain and using Parseval's relation, (1) reduces to

$$\left[\begin{array}{c|c} P & Q \\ \hline R & S \end{array}\right] \begin{bmatrix} a_1 \\ \vdots \\ a_{Mx} \\ b_1 \\ \vdots \\ b_{Mz} \end{bmatrix} = \vec{0} \tag{3}$$

where the matrix elements P, Q, R, and S are given as

$$P_{mn} = \int_{-\infty}^{\infty} \tilde{Y}_{xx} \tilde{e}_m^x \tilde{e}_n^x \, d\alpha \tag{4a}$$

$$Q_{mn} = R_{nm} = \int_{-\infty}^{\infty} \tilde{Y}_{xz} \tilde{e}_m^x \tilde{e}_n^z \, d\alpha \tag{4b}$$

$$S_{mn} = \int_{-\infty}^{\infty} \tilde{Y}_{zz} \tilde{e}_m^z \tilde{e}_n^z \, d\alpha. \tag{4c}$$

The dispersion relation is obtained by solving for values of k_z that render the determinant of the $PQRS$ matrix to zero at a particular wavelength λ_0, substrate thickness d, slot width W, and dielectric constant ϵ_r.

III. Numerical Results and Discussion

The basis functions employed in this paper are

$$e_1^z = U_1\left(\frac{2x}{W}\right)\sqrt{1-\left(\frac{2x}{W}\right)^2} \tag{5a}$$

where U_1 is the Chebyshev polynomial of the second kind of order one

$$e_n^x = T_{2n}\left(\frac{2x}{W}\right)\Big/\sqrt{1-(2x/W)^2} \tag{5b}$$

where $T_{2n}(x)$ are Chebychev polynomials of the first kind of even order.

The longitudinal (z-directed) component is an odd function of x, whereas the transverse (x-directed) component is an even function of x, which would be the field configuration for the fundamental mode on the slot. Since the longitudinal component

TABLE I
COMPARISON OF MEASURED AND CALCULATED SLOT WAVELENGTHS

W/d	Frequency (GHz)	(d/λ_0)	(W/λ_0)	Measured (λ'/λ_0)	Calculated (λ'/λ_0)	% Error
1.335						
	2.0	0.0103	0.014	0.8726	0.8885	+1.39
	2.5	0.0129	0.0175	0.86632	0.8834	+1.5
	3.0	0.0155	0.021	0.8623	0.879	+1.9
	3.5	0.0181	0.0245	0.8516	0.875	+2.0
	4.0	0.021	0.028	0.8667	0.871	+0.39
10.71						
	2.0	0.0103	0.1107	0.9333	0.958	+2.64
	2.5	0.0129	0.1383	0.9375	0.954	+1.82
	3.0	0.0155	0.166	0.945	0.951	+0.66
	3.5	0.0181	0.1937	0.9333	0.948	+1.57
	4.0	0.021	0.22	0.9289	0.943	+1.5
	5.0	0.0258	0.277	0.9215	0.939	+1.89
	6.0	0.031	0.332	0.9156	0.933	+1.8

$\epsilon_r = 2.55$, $d = 1.57$ mm (0.062 in)

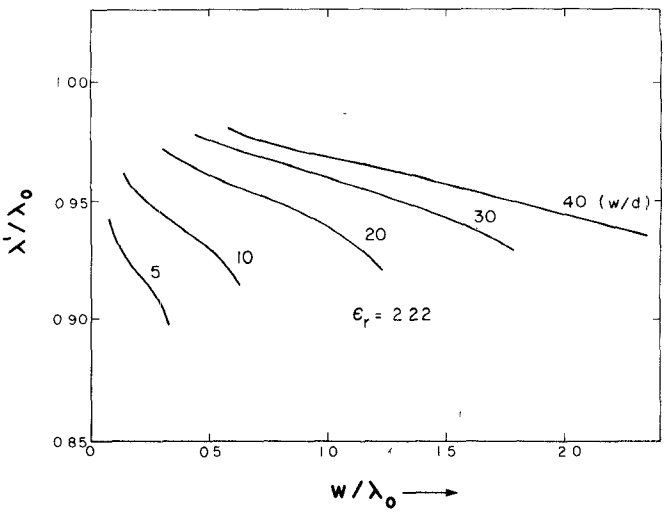

Fig. 3. Normalized slot wavelength as a function of slot width.

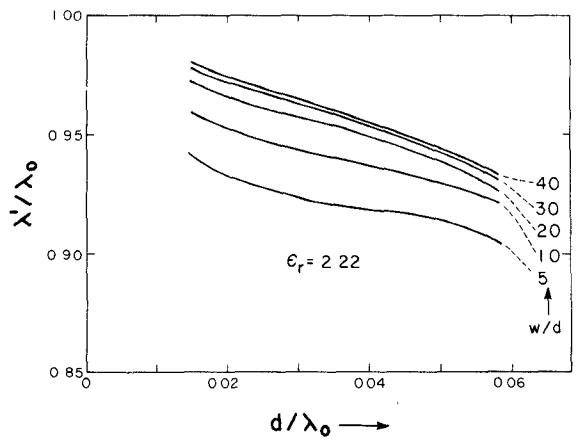

Fig. 4. Normalized slot wavelength as a function of substrate thickness.

is an order of magnitude less than the transverse component [4], only one basis function is considered for the z-component. The Fourier transforms of the basis functions are available in closed form as [11]

$$\tilde{e}_1^z = j2\left(\frac{\pi W}{2}\right)\frac{J_2\left(\frac{\alpha W}{2}\right)}{\left(\frac{\alpha W}{2}\right)}$$

$$\tilde{e}_n^x = (-1)^n\left(\frac{\pi W}{2}\right)J_{2n}\left(\frac{\alpha W}{2}\right), \qquad n = 0,1,\cdots.$$

The integrals in (4) must be evaluated numerically. However, the choice of basis functions in (5) facilitates the extraction of the asymptotic contribution of the integrals and converts them to rapidly convergent integrals suitable for efficient numerical computation. This procedure reduces the CPU time required for computing the integrals in (4) by a factor of about 10. The CPU time taken for the computation of the integrals for a particular value of m, n is around 15 s on a VAX 11/750 minicomputer. The zero of the determinant of the matrix in (3) is found by an iterative technique. It is found that the solution was convergent with 3–4 modes for the transverse component and that the solution can be obtained in seven iterations. For narrow slots, sufficiently accurate results are obtained with only one transverse basis function.

The slot wavelength λ' has been computed for four substrates with $\epsilon_r = 2.22$, 3.0, 3.8, and 9.8 and for slot widths $0.005 \leqslant W/\lambda_0 \leqslant 2.0$. The thickness of the substrate (d/λ_0) over which these computations have been carried out ranged between 0.006 and 0.06. Computed values of the normalized slot wavelength versus the width of the slot are plotted in Fig. 2. Comparison of the normalized wavelength between the present calculations and those in [2] over $0.02 \leqslant d/\lambda_0 \leqslant 0.07$, for $\epsilon_r = 9.6$ and $w/d = 2.0$, showed that the two agree to within 1 percent. Experiments were carried out on a 1.57-mm (0.062-in) substrate ($\epsilon_r = 2.55$) over 2–6 GHz to validate the computed data. The slot wavelength λ' was measured using the scheme suggested in [1]. Table I shows the comparison between theory and experiment for a narrow slot and a wide slot. It is seen that the two results agree to within 2.0 percent over most of the frequency range.

The dispersion curves asymptotically approach the TE_0 surface wave wavelength in the limit of a wide slot at any particular substrate thickness. That this is the case can be shown analytically by considering basis functions without the edge condition and passing the limit on the determinant in (3). The sensitivity of the dispersion characteristics with respect to the slot width W/λ_0 and substrate thickness d/λ_0 is shown in Figs. 3 and 4 for $\epsilon_r = 2.22$. At a fixed frequency, the substrate thickness has a greater effect on the guide wavelength than does the slot width. This can be verified by considering the curves in Fig. 2(a). Starting from any point on the $d/\lambda_0 = 0.015$ curve, the decrease in λ' caused by doubling d (moving to the $d/\lambda_0 = 0.029$ curve at the same W/λ_0) is greater than the increase in λ' caused by moving along the $d/\lambda_0 = 0.015$ curve to the point where W is twice its original value. This effect produces the negative slope in the curves of Figs. 3 and 4, which show λ'/λ_0 as W and d are simultaneously increased.

IV. CONCLUSION

A spectral-domain Galerkin method is used to compute the dispersion characteristics of wide slotlines on low-permittivity substrates that are electrically thin. The choice of expansion and testing functions permits extraction of the asymptotic form of the infinite integrals, resulting in a computationally efficient solution. The agreement between calculated and measured slot wavelengths on narrow and wide slots is generally within 2.0 percent over 2–6 GHz.

REFERENCES

[1] S. B. Cohn, "Slot line on a dielectric substrate," *IEEE Trans. Microwave Theory Tech.*, vol. MTT-17, pp. 768–778, Oct 1969.

[2] E. A. Mariani *et al*, "Slot line characteristics," *IEEE Trans. Microwave Theory Tech.*, vol. MTT-17, pp. 1091–1096, Dec. 1969.

[3] T. Itoh and R. Mittra, "Dispersion characteristics of slot lines," *Electron. Lett*, vol. 7, pp. 364–365, July 1971.

[4] J. B. Knorr and K. Kuchler, "Analysis of coupled slots and coplanar strips on dielectric substrate," *IEEE Trans. Microwave Theory Tech.*, vol. MTT-23, pp. 541–548, July 1975.

[5] R. Garg and K. C. Gupta, "Expressions for wavelength and impedance of a slot line," *IEEE Trans. Microwave Theory Tech.*, vol. MTT-24, pp. 532, Aug. 1976.

[6] J. B. Davies and D. Mirshekar-Syahkal, "Spectral domain solution of arbitrary coplanar transmission line with multilayer substrate," *IEEE Trans. Microwave Theory Tech.*, vol. MTT-25, pp. 143–146, Feb. 1977.

[7] E. L. Kollberg *et al.*, "New results on tapered slot endfire antennas on dielectric substrate," presented at 8th IEEE Int. Conf. on Infrared and millimeter waves, Miami, Dec. 1983.

[8] K. S. Yngvesson, "Near-millimeter imaging with integrated planar receptors: General requirements and constraints," in *Infrared and Millimeter Waves*, vol 10, K. J. Button. Ed. New York: Academic Press.

[9] S. N. Prasad and S. Mahapatra, "A new mic slot-line aerial," *IEEE Trans. Antennas Propagat*, vol AP-31, no. 3, pp. 525–527, May 1983.

[10] T. Itoh, "Spectral domain immitance approach for dispersion characteristics of generalized printed transmission lines," *IEEE Trans. Microwave Theory Tech.*, vol. MTT-28, pp. 733–736, July 1980.

[11] A. Erdelyi, *Tables of Integral Transforms*, vol. 2. New York: McGraw-Hill, 1954.

Transient Analysis of Microstrip Gap in Three-Dimensional Space

SHOICHI KOIKE, NORINOBU YOSHIDA, AND ICHIRO FUKAI

Abstract — **In this paper, we deal with the microstrip gap that should be analyzed in three-dimensional space. The time variations of the electric field at each surface of the stripline having a finite metallization thickness are analyzed. Our method of analysis is based on both an equivalent circuit of Maxwell's equations and Bergeron's method. The former has advantages in the vector analysis by using all electromagnetic components. The latter has advantages in the time-domain analysis of the field. Therefore, our method can analyze field variations in three-dimensional space and time. We present the time variation of the instantaneous electric-field distributions below the strip, at the side of the strip, and at the gap end surface. These results show how the steady-state field distribution grows in the gap.**

I. INTRODUCTION

The microstrip gap is important as a coupling component in MIC [1], [2]. In this paper, we analyze the microstrip gap in three-dimensional space [3]. The transient analysis of the electromagnetic field is not only useful in clarifying the field response but also yields information on the mechanism by which the distribution of the electromagnetic field in the stationary state is brought about. We have recently proposed a new numerical method for the transient analysis of the electromagnetic field in three-dimensional space by formulating the equivalent circuit which simulates Maxwell's equations by Bergeron's method [4], [5]. We analyze the microstrip gap with this method, taking into account the thickness of the strip conductor. This paper presents the time variation of the instantaneous electric-field distributions below the strip, at the side of the strip, and at the gap end surface. These results show how the steady-state field distribution grows in the gap.

Manuscript received November 27, 1984; revised March 18, 1985.

The authors are with the Faculty of Engineering, Hokkaido University, Sapporo, 060 Japan.

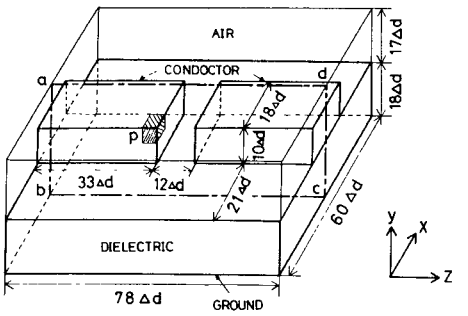

Fig. 1. Model of microstrip gap.

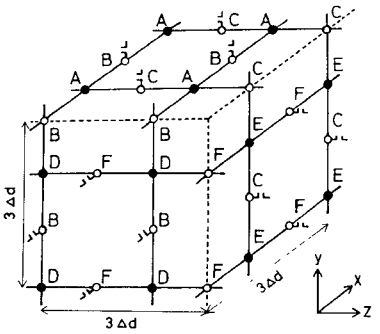

Fig. 2. Arrangement of nodes on the surfaces of the conductor.

II. ANALYZED MODEL OF THE MICROSTRIP GAP

In Fig. 1, the model of the microstrip gap is shown. In this figure, Δd is the interval between adjacent nodes in the equivalent circuit, and the plane *abcd* is a plane of symmetry with respect to the x-direction. In order to model this structure by Bergeron's method, three principal conditions are introduced, namely the boundary condition at the strip conductor, the boundary condition at the free boundary which is the surface of the analyzed region, and the condition of the dielectric. In this paper, we do not give the details of these formulations. But the boundary condition at the conductor is explained in detail because it is important in the formulation. In this analysis, the conductor is supposed to have infinite conductivity, so the tangential components of the electric field and the normal components of the magnetic field on the surface of the conductor should be zero. For example, the equivalent circuit of the part designated by p on the strip conductor in Fig. 1 is presented in Fig. 2. In this figure, the notations ●, ○, and ⊣ represent the electric node in which the voltage variable corresponds to the electric-field component, the magnetic node in which the voltage variable corresponds to the magnetic-field component, and the open-circuit condition, respectively. So the equivalent circuit for the surface of the conductor is realized by: 1) short-circuiting the node on the surface, in which the tangential component of the electric field or the normal component of the magnetic field corresponds to the voltage variable; 2) open-circuiting the node, in which the preceding electromagnetic component corresponds to a current variable. Fig. 2 shows the resultant equivalent circuit obtained by the above-mentioned treatment of the boundary

0018-9480/85/0800-0726$01.00 ©1985 IEEE